Pergamon

Bioorganic & Medicinal Chemistry Letters 12 (2002) 2109–2112

BIOORGANIC & MEDICINAL CHEMISTRY LETTERS

SAR of 2,6-Diamino-3,5-difluoropyridinyl Substituted Heterocycles as Novel p38 MAP Kinase Inhibitors

Laszlo Revesz,[a,*] Franco E. Di Padova,[a] Thomas Buhl,[a] Roland Feifel,[a] Hermann Gram,[a] Peter Hiestand,[a] Ute Manning,[a] Romain Wolf[a] and Alfred G. Zimmerlin[b]

[a]*Arthritis and Bone Research, Novartis Pharma AG, CH-4002 Basel, Switzerland*
[b]*Preclinical Safety, Novartis Pharma AG, CH-4002 Basel, Switzerland*

Received 5 March 2002; revised 10 May 2002; accepted 13 May 2002

Abstract—2,6-Diamino-3,5-difluoropyridinyl substituted pyridinylimidazoles, -pyrroles, -oxazoles, -thiazoles and -triazoles have been identified as novel p38α inhibitors. Pyridinylimidazole **11** potently inhibited LPS-induced TNFα in mice, showed good efficacy in the established rat adjuvant (ED_{50}: 10 mg/kg po b.i.d.) and collagen induced arthritis (ED_{50}: 5 mg/kg po b.i.d.) with disease modifying properties based on histological analysis of the joints. © 2002 Published by Elsevier Science Ltd.

Introduction

Inhibitors of p38 MAP kinase reduce the production of pro-inflammatory cytokines, e.g., IL-1, TNFα, IFNγ and IL-6, whose excessive production initiates events leading to inflammation and tissue destruction in diseases such as rheumatoid arthritis (RA).[1] p38 Inhibitors not only block the synthesis but also the signal cascades induced by these cytokines;[2] in addition, p38 has been implicated in the induction of COX-2, the inducible prostaglandin cyclooxygenase.[3] The interest in the development of p38 MAP kinase inhibitors is based on the expectations that p38 inhibiting drugs will treat the underlying cause of chronic inflammatory diseases and stop their progression. Previously, we described a series of 4-hydroxypiperidine substituted heterocycles **1**[4] as p38 inhibitors with useful in vivo antiarthritic activities. In search of p38 inhibitors suitable for clinical development we now report new 2,6-diamino-3,5-difluoropyridinyl substituted imidazoles, oxazoles, thiazoles, triazoles and pyrroles **2** and their in vivo efficacies in models of inflammation and rheumatoid arthritis.

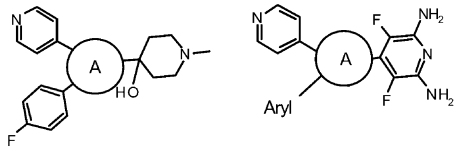

1 **2**

Chemistry

Target compounds with 4-fluorophenyl as aryl substituent in **2** were prepared from imidazole **4**,[4] oxazole **5**,[4] thiazole **6**[4] and bromopyrrole **16**[4] (Scheme 1) involving deprotonation or bromine–lithium exchange with *n*BuLi at −78 °C and reacting the anions with pentafluoropyridine to yield the tetrafluoropyridines **7**–**9** and **17**. The latter were converted with 25% aqueous NH_3 at 150–170 °C to the 2,6-diamino-3,5-difluoropyridines **11**, **13**, **14**, **18** and the 2-amino-3,5,6-trifluoropyridines **10** and **12**.

Triazole **21**—obtained via [3 + 2] cycloaddition reaction of Me_3SiN_3[5] with 4-pyridinylacetylene **20**[6]—was deprotonated with $KN(TMS)_2$ and reacted with pentafluropyridine to the tetrafluoro intermediate **22**, which was transformed into 2,6-diamino-3,5-difluoropyridine **23** (Scheme 2).

A general method for the preparation of a diverse set of aryl substituted pyridinylimidazoles was developed,

*Corresponding author. Tel.: +41-61-324-3231; fax: +41-61-324-3273; e-mail: laszlo.revesz@pharma.novartis.com

0960-894X/02/$ - see front matter © 2002 Published by Elsevier Science Ltd.
PII: S0960-894X(02)00336-0

allowing the introduction of aryl substituents at a late stage of the synthesis (Scheme 3). SEM-protected imidazole **24**[7] was treated with *n*BuLi and the resulting anion arylated with pentafluoropyridine followed by bromination to **25**. 4-Trimethylstannylpyridine[8] and **25** were coupled regioselectively in a Stille reaction, yielding pyridinylimidazole **26**, where the remaining bromine atom served to attach an aryl-substituent either by a Suzuki[9] or a Stille[10] coupling reaction. Removing the SEM-protecting group under acidic conditions and heating in 25% aq NH_3 at 170 °C for 12 h delivered the target compounds **27**–**29** in moderate yields.

Results and Discussion

Molecular modeling suggested,[11,12] that three interactions were the major contributors to the high affinity binding of **1** and **2** to p38α: (a) the hydrogen bridge of the 4-pyridinyl nitrogen to the NH amide of Met109, (b) the 4-fluorophenyl ring extending into a lipophilic pocket near Thr106, (c) the salt bridge between the COOH-group of Asp168 and the basic piperidinyl ring of **1** and the 2,6-diamino-3,5-difluoropyridinyl ring of **2**. Without the possibility to form a salt bridge, unsubstituted imidazole **3**, thiazole **6**, pyrrole **15** and triazole **21** were 6–200-fold less potent than their 2,6-diamino-3,5-difluoropyridinyl analogues **11**, **14**, **19** and **23** (Table 1). Moreover, the stepwise transformation of the 2,3,5,6-tetrafluoropyridinyl into the 2-amino-3,5,6-trifluoropyridinyl and further to the 2,6-diamino-3,5-difluoropyridinyl ring was accompanied by a gradual increase in potency in parallel with the ability to form a salt bridge. Most prominent example were the oxazoles **8** (IC_{50} = 100 μM), **12** (2.1 μM) and **13** (0.4 μM). Interestingly, within the homogenous series of imidazole **11**, oxazole **13**, thiazole **14**, pyrrole **19** and triazole **23**—all with identical substituents on ring **A**—the IC_{50}s differed up to 100-fold with the ranking order of potency: pyrrole **19** (IC_{50} = 4 nM) > imidazole **11** (IC_{50} = 16 nM) > thiazole **14** (IC_{50} = 140 nM) > triazole **23** (IC_{50} = 210 nM) > oxazole **13** (IC_{50} = 400 nM). Assuming, that ring **A** may affect the hydrogen bridge formation to Met109 or the salt bridge formation to Asp168 or both, salt bridge formation may decrease by increasing out-of-plane rotation of the 2,6-diamino-3,5-difluoropyridinyl ring, going from pyrrole **19** to oxazole **13**. While the 2,6-diamino-3,5-difluoropyridinyl ring is assumed to prefer a coplanar conformation with the pyrrole-ring due to F–HN bonding, out-of-plane rotation may gradually increase from thiazole **14**, triazole **23** to the oxazole **13**, thereby rendering salt bridge formation more difficult. An additional effect of ring **A** on the p*K* of the 4-pyridinyl nitrogen can not be excluded. In contrast to earlier findings,[13] where the 4-fluorophenyl group was shown to be optimal in size for the lipophilic binding pocket near Thr106, the 2-benzofuryl analogue **28** (IC_{50} = 5 nM) demonstrates, that larger groups may also be accommodated successfully.

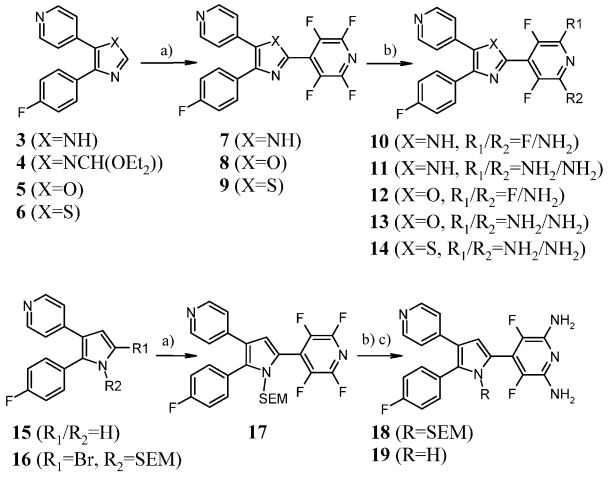

Scheme 1. (a) **4**, *n*BuLi, −78 °C, THF, pentafluoropyridine, 75% **7**, **5**, **6** and **16**: *n*BuLi, −40 °C, THF, pentafluoropyridine, 65% **8**, 54% **9**, and 78% **17**; (b) amination of **7**: autoclave, 25% aq NH_3, 150 °C, 4 h, 44% **10** and 33% **11**. Amination of **8**: 25% aq NH_3, 170 °C, autoclave, 5 h, 18% **12** and 21% **13**. Amination of **9**: 25% aq NH_3, 170 °C, autoclave, 17 h, 34% **14**. Amination of **17**: 25% aq NH_3, 170 °C, autoclave, 17 h, 61% **18**; (c) Bu_4NF, THF, 2.5 h, 60 °C, 75% **19**.

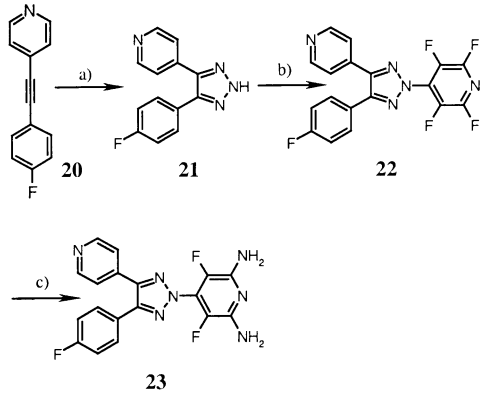

Scheme 2. (a) Me_3SiN_3, autoclave, 130 °C, 48 h, 81%; (b) $KN(TMS)_2$, pentafluoropyridine, THF, 0 °C to room temp, 20 min, 49%; (c) 25% aq NH_3, 170 °C, autoclave, 17 h, 24%.

A selection of compounds in Table 1 with potent inhibition of p38α and TNFα release from LPS-stimulated

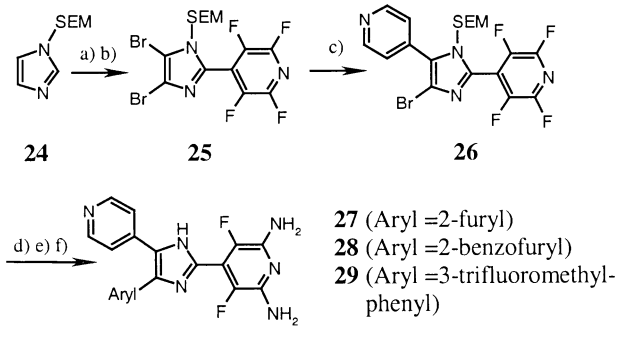

Scheme 3. (a) *n*BuLi, THF, −40 °C, 10 min, −60 °C, pentafluoropyridine, 74%; (b) Br_2, HOAc, NaOAc, 15 min, room temperature, 86%; (c) 4-trimethylstannylpyridine, $PdCl_2(PPh_3)_2$, toluene, reflux 12 h, 46%; (d) 2-(tri-*n*-butylstannyl)furan, $PdCl_2(PPh_3)_2$, xylene, reflux 3 h, 88%. Benzo[b]furan-2-boronic acid, $PdCl_2(PPh_3)_2$, 1,2-dimethoxyethane, Na_2CO_3 aq satd, 100 °C, 1.25 h, 78%. 3-(Trifluoromethyl)phenylboronic acid, 1,2-dimethoxyethane, Na_2CO_3 aq satd, 100 °C, 1.25 h, 92%; (e) EtOH/HCl concd 1:1, room temperature, 1 h, 78–85%; (f) 25% aq NH_3, 170 °C, autoclave, 12 h, 30–36%.

Table 1.

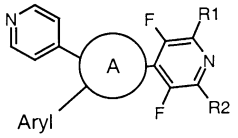

	Aryl	A	R_1/R_2	p38α[a,14]	TNFα[b,15]	COX-1[a,16]
3	4-Fluorophenyl	Imidazole	[c]	1.00	n.t.	n.t.
6	4-Fluorophenyl	Thiazole	[c]	0.80	n.t.	n.t.
7	4-Fluorophenyl	Imidazole	F/F	0.09	0.074	>100
8	4-Fluorophenyl	Oxazole	F/F	100	n.t.	n.t.
10	4-Fluorophenyl	Imidazole	F/NH_2	0.004	0.044	100
11	4-Fluorophenyl	Imidazole	NH_2/NH_2	0.016	0.044[d]	>100
12	4-Fluorophenyl	Oxazole	F/NH_2	2.1	1.93	100
13	4-Fluorophenyl	Oxazole	NH_2/NH_2	0.4	0.373	100
14	4-Fluorophenyl	Thiazole	NH_2/NH_2	0.14	0.031	100
15	4-Fluorophenyl	Pyrrole	[c]	0.80	n.t.	n.t.
19	4-Fluorophenyl	Pyrrole	NH_2/NH_2	0.004	0.018	6.3
21	4-Fluorophenyl	Triazole	[c]	1.30	n.t.	n.t.
22	4-Fluorophenyl	Triazole	F/F	10	n.t.	10
23	4-Fluorophenyl	Triazole	NH_2/NH_2	0.21	n.t.	45
27	2-Furyl	Imidazole	NH_2/NH_2	0.67	0.294	100
28	2-Benzofuryl	Imidazole	NH_2/NH_2	0.005	0.027	100
29	3-Trifluoromethylphenyl	Imidazole	NH_2/NH_2	0.47	0.054	100

[a]IC_{50} (μM).
[b]IC_{50} (μM) of TNFα release from LPS-stimulated human peripheral blood mononuclear cells.
[c]Not applicable.
[d]IC_{50} = 0.25 μM for TNFα release inhibition from LPS-stimulated human whole blood.

Table 2.

	TNFα[a]	AIA[b]	CIA; ED_{50} (po)[c]
7	3	n.t.	n.t.
10	64	71 (toxic)	n.t.
11	83	ED_{50}:10 mg/kg bid	5 mg/kg b.i.d. 43 mg/kg q.d.
13	81	19	n.t.
27	28	n.t.	n.t.
28	1.8	n.t.	n.t.
29	21	n.t.	n.t.

[a]% Inhibition of LPS induced TNFα release in mice[17] at 10 mg/kg po.
[b]% Inhibition of swelling in adjuvant induced arthritis rats[18] (AIA) at 25 mg/kg po b.i.d.
[c]CIA, collagen induced arthritis in rats.[19] Inhibition of paw-swelling.

human peripheral blood mononuclear cells were tested in vivo for their antiarthritic profile. Compounds with IC_{50} <10 μM against COX-1 were excluded due to unacceptable ulceration risks.

10, **11** and **13** (Table 2) were found to have antiarthritic potential; they inhibited TNFα release by 60–80% at a dose of 10 mg/kg po in the mouse[17] and were further tested in the established adjuvant induced arthritis model in the rat (AIA)[18] at a dose of 25 mg/kg po b.i.d. Imidazole **10** inhibited paw-swelling by 71%, but was not well tolerated. Oxazole **13** gave only a modest inhibition of 19%, which was insufficient for further investigations. Imidazole **11** was the most potent analogue in vivo with inhibition of LPS-induced TNFα in mice (Table 2) and rats (ED_{50} = 4 mg/kg po).

11 inhibited paw swelling in established models of arthritis with ED_{50}s of 10 mg/kg b.i.d. po (AIA[18]) and 5 mg/kg b.i.d. po (CIA[19]).

Histological evaluation of hind paws from CIA-rats revealed a dose-dependent protective activity of **11** (at 3, 10, 30 mg/kg po b.i.d.) on bone apposition (−4, −44, −64%), loss of proteoglycans (−17, −38, −42%), cartilage damage (−15, −44, −58%) and infiltration of cells (−11, −37, −45%), pointing to a disease modifying potential of **11** in rheumatoid arthritis. The compound also showed an acceptable kinase selectivity profile,[20] and satisfactory pharmacokinetic properties in the rat (bioavailability: 49%; $t_{1/2}$: 1 h; C_{max}: 3.12 μM @ 10 mg/kg po). Pyridinylimidazole inhibitors of p38α often risk to inhibit CYP450 isoenzymes by coordinating their 4-pyridinyl nitrogen to the heme iron. Increased liver weight and significant elevations of hepatic P450 isoenzymes by SB203580—a representative of this structure class—were stated to be related to P450-inhibition.[23] Pyridinylimidazole **11** was devoid of human P450 inhibition. [Isoenzyme: IC_{50} (μM); CYP1A2: >100; CYP2C9: 65.5; CYP2D6: >100; CYP3A4: >100].[24]

In conclusion, a series of 2,6-diamino-3,5-difluoropyridinyl substituted pyridinylimidazoles, -pyrroles, -oxazoles, -thiazoles and -triazoles has been identified as novel p38α inhibitors. Imidazole **11** from this series showed potent disease modifying antiarthritic properties in AIA and CIA models.

Acknowledgements

We would like to thank E. Blum and G. Rucklin for excellent technical assistance, W. Prikoszovich, F. Struber and B. Wietfeld for the large scale preparation of **11** and Prof. W. van den Berg (Nijmwegen) for the histological evaluation.

References and Notes

1. Adams, J. L.; Badger, A. M.; Kumar, S.; Lee, J. C. *Prog. Med. Chem.* **2001**, *38*, 1.
2. Kumar, S.; McDonnell, P. C.; Gum, R. J.; Hand, A. T.; Lee, J. C.; Young, P. R. *Biochem. Biophys. Res. Commun.* **1997**, *235*, 533.
3. Lee, J. C.; Blumenthal, M. J.; Laydon, J. T.; Tan, K. B.; DeWitt, D. L. 7th International Conference of the Inflammatory Research Association, Poconos, PA, 1994. Lin, W. W.; Chen, B. C. *Br. J. Pharmacol.* **1999**, *126*, 1419.
4. Revesz, L.; Di Padova, F. E.; Buhl, T.; Feifel, R.; Gram, H.; Hiestand, P.; Manning, U.; Zimmerlin, A. G. *Bioorg. Med. Chem. Lett.* **2000**, *10*, 1261. Revesz, L. WO 9901449, 1999; *Chem. Abstr.* **1999**, *130*, 125072.
5. Birkofer, L.; Wegner, P. *Chem. Ber.* **1966**, *99*, 2512.
6. Zablocki, J. A.; Tarlton, E., Jr.; Rizzi, J. P.; Mantlo, N. B. WO 9822457, **1998**; *Chem. Abstr.* **1998**, *129*, 27933.
7. Whitten, J. P.; Matthews, D. P.; McCarthy, J. R. *J. Org. Chem.* **1986**, *51*, 1891.
8. Yamamoto, Y.; Azuma, Y.; Mitoh, H. *Synthesis* **1986**, *7*, 564.
9. Miyaura, N.; Suzuki, A. *Chem. Rev.* **1995**, *95*, 2457.
10. Stille, J. K. *Angew. Chem., Int. Ed. Engl.* **1986**, *25*, 508.
11. Shewchuk, L.; Hassell, A.; Wisely, B.; Rocque, W.; Holmes, W.; Veal, J.; Kuyper, L. F. *J. Med. Chem.* **2000**, *43*, 133.
12. Lisnock, J. M.; Tebben, A.; Frantz, B.; O'Neill, E. A.; Croft, G.; O'Keefe, S. J.; Li, B.; Hacker, C.; de Laszlo, S.; Smith, A.; Libby, B.; Liverton, N.; Hermes, J.; LoGrasso, P. *Biochemistry* **1998**, *37*, 16573.
13. Liverton, N. J.; Butcher, J. W.; Claiborne, C. F.; Claremon, D. A.; Libby, B. E.; Nguyen, K. T.; Pitzenberger, S. M.; Selnick, H. G.; Smith, G. R.; Tebben, A.; Vacca, J. P.; Varga, S. L.; Agarwal, L.; Dancheck, K.; Forsyth, A. J.; Fletcher, D. S.; Frantz, B.; Hanlon, W. A.; Harper, C. F.; Hofsess, S. J.; Kostura, M.; Lin, J.; Luell, S.; O'Neill, E. A.; Orevillo, C. J.; Pang, M.; Parsons, J.; Rolando, A.; Sahly, Y.; Visco, D. M.; O'Keefe, S. J. *J. Med. Chem.* **1999**, *42*, 2180.
14. A phosphorylated form of His-p38α MAP kinase (10 ng/well) of murine origin was used and immobilised GST-ATF-2 as substrate in the presence of 120 μM cold ATP.
15. Human peripheral blood mononuclear cells from healthy volunteers were incubated with the inhibitor and stimulated with LPS/IFN-γ for 3 h. The supernatants were collected for TNF-α determination by ELISA.
16. COX-1 from ram seminal vesicles (No. 60100; Cayman Chemical Company) was used and PGE2 determined by RIA.
17. 8-week old female OF1 mice were dosed perorally by gavage with solutions of the compounds in DMSO/cornoil. 1 h after dosing, LPS (20 mg/kg) was injected iv for stimulation of TNF-α release into plasma. 1 h later, blood was collected and TNFα was determined using a mouse specific ELISA.
18. AIA: Adjuvant induced arthritis. Female Wistar rats were immunised with Mycobacterium tuberculosis at day 0 and dosed with the compounds (2×25 mg/kg po per day) from day 14 to day 20. Swelling of the joints was measured on day 20.
19. CIA: Collagen induced arthritis. Female (WAGxBUF/F1) rats were immunised intradermally with bovine nasal septum type II collagen emulsified in Freund's incomplete adjuvant. Swelling started ~10 days after immunisation. Dosing of compounds started on day 13, when swelling was nearly maximal. **11** was dosed once (q.d.) or twice (b.i.d.) daily for 10 days.
20. Kinase selectivity profile of **11**. Kinase; IC_{50} (μM). **p38β2**[21] (0.057); **p38δ**[21] (>10); **JNK1**[21] (7.22); **JNK2**[21] (0.202); **PKCα**[22] (>100); **ERK2**[22] (>10); **MKK6b**[22] (85.33); **EGFR**[22] (1.339); **c-abl**[22] (56.3); **c-src**[22] (>100).
21. Phosphorylated forms of His-p38β2, His-p38δ, His-JNK1 and His-JNK2 MAP kinases of human origin phosporylated the immobilised substrate GST-ATF-2 in the presence of cold ATP (120 μM). Antibody detected phosphorylated GST-ATF-2.
22. A phosphorylated form of murine ERK2 MAP kinase phosphorylated a peptide in the presence of cold and 0.1 μCi of (^{32}P)γ-ATP. MKK6b(EE) kinase: An active form of GST-MKK6b(EE) of human origin phosporylated the immobilised substrate GST-p38α(K>M) in the presence of cold ATP (12 μM). EGFR kinase: purified human EGFR-ICD, 400 nM cold ATP, poly (EY) as substrate and 0.1 μCi of (^{32}P)γ-ATP. C-abl: murine enzyme, cold ATP (5 μM), poly(AEKY) as substrate and 0.06 μCi of (^{32}P)γ-ATP. C-src: activated chicken kinase 20 μM, cold ATP, poly (EY) as substrate and 0.07 μCi of (^{32}P)γ-ATP. PKCα: bovine kinase, 10 μM cold ATP, substrate protamine sulfate and 0.1 μCi of (^{32}P)γ-ATP.
23. Adams, J. L.; Boehm, J. C.; Kassis, S.; Gorycki, P. D.; Webb, E. F.; Hall, R.; Sorenson, M.; Lee, J. C.; Ayrton, A.; Griswold, D. E.; Gallagher, T. F. *Bioorg. Med. Chem. Lett.* **1998**, *8*, 3111.
24. Crespi, C. L.; Miller, V. P.; Penman, B. W. *Anal. Biochem.* **1997**, *248*, 188.